Acta Crystallographica Section B
Structural Science, Crystal Engineering and Materials
ISSN 2052-5192

Isoelectronic and isolobal O, CH_2, CH_3^+ and BH_3 as electron pairs; similarities between molecular and solid-state chemistry

Ángel Vegas,[a,b]* Rafael Notario,[b]* Eduardo Chamorro,[c] Patricia Pérez[c] and Joel F. Liebman[d]

[a]Universidad de Burgos, Parque Científico y Tecnológico, Edificio I+D+I, Plaza Misael Bañuelos s/n, 09001 Burgos, Spain, [b]Instituto de Química Física Rocasolano, CSIC, Serrano 119, 28006 Madrid, Spain, [c]Departamento de Ciencias Químicas, Facultad de Ciencias Exactas, Universidad Andres Bello (UNAB), Avda. República 275, 837-0146 Santiago, Chile, and [d]Department of Chemistry and Biochemistry, University of Maryland, Baltimore County, 1000 Hilltop Circle, Baltimore, MD 21250-1000, USA

Correspondence e-mail: avegas@iqfr.csic.es, rnotario@iqfr.csic.es

Received 27 November 2012
Accepted 11 January 2013

A topological analysis of the electron localization function (ELF) of a molecule of hexamethyldisiloxane, $(H_3C)_3$–Si–O–Si–$(CH_3)_3$, has been carried out, drawing a consistent picture of Si—O—Si bonding both in the linear and angular geometries. The ELF analysis confirms the idea that the O atom, in the linear geometry of $(H_3C)_3$—Si—O—Si—$(CH_3)_3$, is isolobal with the isoelectronic $-CH_3^+-$ and $-BH_3-$ groups, the bonding in the Si—O—Si group being described as a two-electron, three-center ($2e$, $3c$) bond. At the same time, the three oxygen lone pairs mirror the three C—H and B—H bonds, respectively. On the contrary, in the angular geometry the same O atoms form two Si—O bonds and its lone pairs mimic the geometry of the $-CH_2-$ group. In this model the O atoms would play the same role as the formally present O^{2-} anions in the 'so-called' ionic solids, such as in the skeletons of aluminate and silicate polyanions, thereby connecting molecular and solid-state chemistry as formulated by the 'fragment formalism' or the 'molecular unit-cell approach'. This unifying concept as well as the calculations we have carried out fully agree and also give support to earlier ideas developed by Bragg and Bent, among other authors. Bonding in the series of compounds P_4, P_4O_6, P_4O_{10}, $N_4(CH_2)_6$ (hexamethylenetetramine) and $(CH)_4(CH_2)_6$ (adamantane) is discussed in the context of the isolobal model.

1. Introduction

In 1974 Klevan and Munson (Klevan & Munson, 1974) reported for the first time the formation of the carbocation $[(H_3C)_3—Si—CH_3—Si—(CH_3)_3]^+$ [hereafter (I^+)] as an ion–molecule reaction product of tetramethylsilane in the gas phase under high-pressure conditions [0.3 Torr; see (1)].

$$Si(CH_3)_3^+ (g) + Si(CH_3)_4 (g) \rightarrow Si_2(CH_3)_7^+ (g) \qquad (1)$$

Further investigations carried out by Wojtyniak *et al.* (1987) and by Stone (1997), using high-pressure mass spectrometry, confirmed the existence of that ion, and the same process was applied to synthesize analogous Ge and Sn derivatives.

Very recently, Dávalos *et al.* (2007) have reported that, under pressures as low as 10^{-8}–10^{-5} mbar, the kinetic excitation of $Si(CH_3)_3^+$ by means of on-resonance irradiation or slightly off-resonance irradiation (SORI) under multiple-collision conditions, increases the yield of (I^+) (Laskin *et al.*, 2000). In that work, the structure of (I^+) was optimized by quantum chemical calculations at the QCISD/6-311+G(d,p) level of theory. As can be observed in Fig. 1, the molecule has C_3 symmetry with its central C atom (penta-coordinated) occupying the center of a trigonal bipyramid, with the three H atoms at the equatorial plane and the two Si atoms at the apical positions. This charged species could be regarded as a

CH_3^+ cation interacting with two $(CH_3)_3Si^\bullet$ radicals (Dávalos *et al.*, 2007).

As the central C atom (CH_3^+ cation) has only three valence electrons, shared with the H atoms, the C and the two Si atoms must form a two-electron, three-center bond (Dávalos *et al.*, 2007). Theoretical works (Jemmis *et al.*, 1979; Fernández *et al.*, 2007) have shown the stability of penta-coordinated carbenium ions and other cations containing more electropositive elements than carbon (Be and Group 13 and 14 elements) and whose bonding scheme also fits to a (2*e*, 3*c*) bond.

Before we proceed, we acknowledge that some readers may be disturbed that we will employ conflicting ways of understanding chemical thought, isolobal reasoning and valence-shell electron-pair repulsion (VSEPR), discussing gas-phase ions, discrete molecular entities and crystalline solids, traversing inorganic, organometalloid and organometallic, organic chemistry. Let us try to assuage this by simply recalling the content and the related philosophy of the recent papers 'Does the death knell toll for the metallic bond?' (Schön, 1995), 'The metallic bond – dead or alive? A comment' (Allen & Burdett, 1995) and 'A conversation on VB *versus* MO theory: a never-ending rivalry?' (Hoffmann *et al.*, 2003). We note an additional sense of disquiet. It is not uncommon that when a new concept arises with vestiges of earlier seemingly disparate and incompatible ideas, different sounding words are used to describe the new models of understanding. For example, explicitly bridging the molecular and solid-state sciences are the related 'molecular unit-cell approach' (Messmer *et al.*, 1972; Messmer & Watkins, 1973) and the 'small-periodic cluster technique' (Zunger, 1974*a*,*b*, 1975). Particularly evocative studies using the 'fragment formalism' are Burdett & Lin (1981, 1982) wherein bands and bonds, VSEPR models and MO pictures, molecules, parts of molecules, and 'infinite' crystals comfortably and indeed synergistically and symbiotically coexist.

Returning now to the molecular geometry of the (I^+) cation, the linearity of the Si—C—Si bond is a consequence of the electron deficiency of the bridging CH_3^+ group. However, it should be emphasized that this charged group is isoelectronic with a neutral O atom (6 valence electrons). If this observation is linked to the isolobal concept, developed by Hoffmann (1982), one could expect the existence of similar compounds where bridging an O atom replaces the CH_3^+ group. This is the case for organic molecules like dimethyl ether H_3C–O–CH_3, the many silicate and related Al-, Si- and P-containing polyanions such as $[Si_2P_6O_{25}]^{12-}$ and also most of the SiO_2 polymorphs, such as quartz, cristobalite, tridymite, coesite and keatite.

An important feature is that in some compounds (aluminates, silicates) the Si–O–Si group is linear like in the anion $[Si_2P_6O_{25}]^{12-}$ of both $Mo_4[Si_2P_6O_{25}]$ (Leclaire *et al.*, 1988) and $In_4[Si_2P_6O_{25}]$ (Hanawa *et al.*, 2000), and in the $[Si_2O_7]^{6-}$ anion in thortveitite $Sc_2Si_2O_7$ (Cruickshank *et al.*, 1962; see Fig. 2), whereas in other silicates it adopts an angular geometry. The same occurs in the silica polymorphs. In quartz, cristobalite and keatite the Si—O—Si groups are bent whereas in tridymite and in the high-pressure phase coesite, they are linear. The most frequent value for the Si—O—Si angle is in the range 145–150° (O'Keeffe & Hyde, 1981). It is pertinent to recall here how the traditional cubic structure assigned to

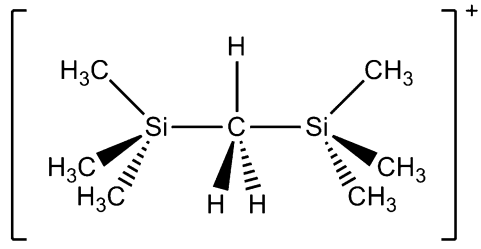

Figure 1
Structure of $Si_2(CH_3)_7^+$ (I^+).

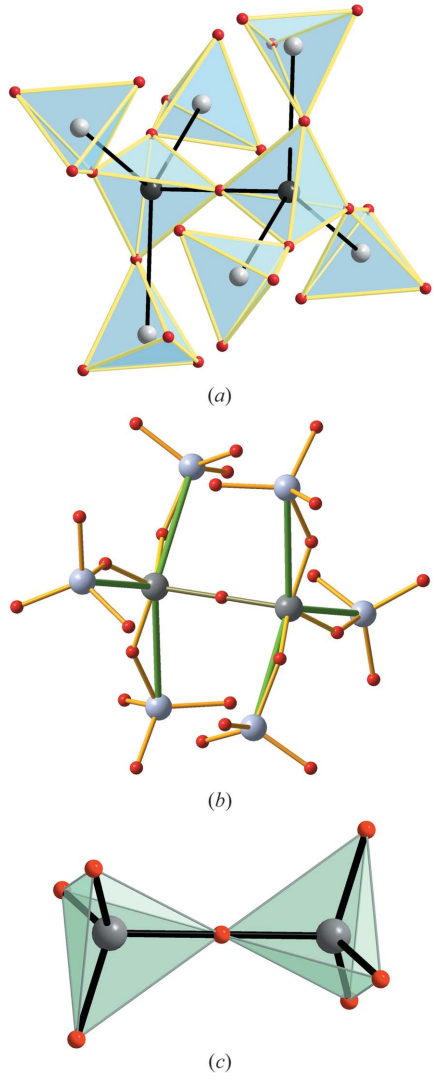

Figure 2
Two views of the structure of the $[(O_3PO)_3Si—O—Si(OPO_3)_3]^{12-}$ polyanion in both (*a*) $In_4[Si_2P_6O_{25}]$ and (*b*) $Mo_4[Si_2P_6O_{25}]$, showing the linear Si—O—Si bond and the six angular Si—O—P bonds. On the left, the solid SiO_4 and PO_4 tetrahedra have been explicitly depicted (Si: black, P: light grey, O: small and medium grey). On the right, Si: dark-grey, P: light-grey, O: red; the Si—Si and Si—P contacts are also drawn. In (*c*) the $[Si_2O_7]^{6-}$ anion in $Sc_2Si_2O_7$ is depicted to show the linearity of the Si—O—Si group.

cristobalite ($Fd\bar{3}m$), implying linear Si—O—Si groups, was erroneous. Instead, the structure redetermination, carried out by Dollase (1965), led to the correct tetragonal structure ($P4_12_12$) containing angular Si–O–Si groups.

This variable behaviour of the O atom that bridges two Si(C) atoms makes the following assumption: If the O atom was isolobal with both $-CH_2-$ and $-CH_3^+-$, then we might establish a correspondence between the angular molecules $H_3C-CH_2-CH_3$ and $H_3C-O-CH_3$, on one hand, and between the linear species $[(H_3C)_3-Si-CH_3-Si-(CH_3)_3]^+$ (I^+) and $(H_3C)_3-Si-O-Si-(CH_3)_3$ on the other hand.

In the case of the angular molecules, because the central atom (C or O) forms covalent two-electron bonds with the neighboring C atoms, the spatial distribution of the oxygen lone pairs in dimethyl ether should correspond to that of the C—H bonds in the central CH_2 group in propane. On the contrary, in the linear molecules the three equatorial C—H bonds formed by the central C atom (see Fig. 1) would consider the view of the linear Si—C—Si group as a two-electron, three-center bond. This idea should be consistent with the preferred geometries given within the VSEPR model (Gillespie & Popelier, 2001) as has been pointed out by Papoian & Hoffmann (2000).

If we intend to create a bonding pattern for the $(H_3C)_3-Si-O-Si-(CH_3)_3$ molecule (hexamethyldisiloxane), isolobal to (I^+), we have two possibilities, which are schematized in Fig. 3. The first one contemplates the formation of an angular molecule and should be an extension of the model applied to the ether molecule, with two O lone pairs playing the role of the CH_2 group in propane. The second model leads to the formation of a linear molecule, in which the bonding pattern would fit the electron distribution in (I^+), that is, one (2*e*, 3*c*) bond involving the Si—O—Si atoms and the remaining six valence electrons of the O atom forming three lone pairs at the equatorial plane like the three C—H bonds of the central CH_3^+ group in (I^+).

As has been clearly pointed out by Hoffmann (1982), two isolobal moieties do not necessarily have to be isostructural or isoelectronic. However, the isolobal character of both the CH_2 moiety and the O atom seems evident in molecules such as $H_3C-CH_2-CH_3$ and $H_3C-O-CH_3$, and the small-ring species cyclopropane and ethylene oxide. Very recently, the isoelectronic and isolobal relationship between the methylene group and bridging O atoms has been used as a tool for the synthesis of a methylene derivative of the layer silicate saponite using bis(triethoxysilyl)methane as an organosilicon reagent (Xue & Pinnavaia, 2010).

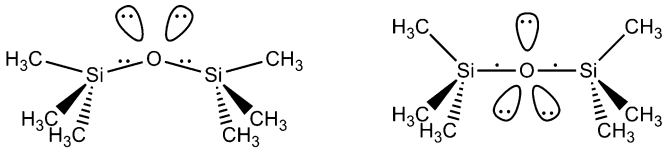

Figure 3
The two bonding models for the $(H_3C)_3-Si-O-Si-(CH_3)_3$ molecule (hexamethyldisiloxane), explicitly showing the bonding electrons and lone pairs.

The molecule SF_4 (34 electrons in the valence shell) (Mootz & Korte, 1984) and the isoelectronic $[PbO_4]^{6-}$ fragment separated from the red PbO structure (Moore & Pauling, 1941), provide a nice example of the small-periodic cluster technique (Zunger, 1974*a*,*b*, 1975). Both moieties, SF_4 and $[PbO_4]^{6-}$ are isoelectronic, isolobal and isostructural in spite of their molecular or extended solid character, respectively (Burdett & Lin, 1981, 1982). The structures are represented in Fig. 4.

The structure of SF_4 obtained at 152.2 K by Mootz & Korte (1984) exhibits positional disorder of the F atoms, but one of the present conformations agrees with the square-pyramidal conformer suggested by Burdett & Lin (1981) and drawn in Fig. 4.

Now, the question that arises is whether the linear array of the Si—O—Si group might provoke the central O atom to become isolobal with the CH_3^+ group in (I^+): we recall a comparison of ethylene oxide and protonated cyclopropane (Dewar & Ford, 1979). To elucidate this problem, we have undertaken theoretical calculations, including the electron localization function ELF.

2. Theory and computational details

The electron localization function (ELF) is a relative local measure of the *same spin pair density distribution*, *i.e.* it measures the Pauli repulsion at a given spatial position (Becke & Edgecombe, 1990; Savin *et al.*, 1991, 1997; Silvi, 2002). Conveniently defined, ELF values close to 1 are associated with regions with a high probability of *electron pairing*. Although originally introduced in the context of single-determinant (Hartree–Fock) wavefunctions (Becke & Edgecombe, 1990; Savin *et al.*, 1997), the analysis and interpretation

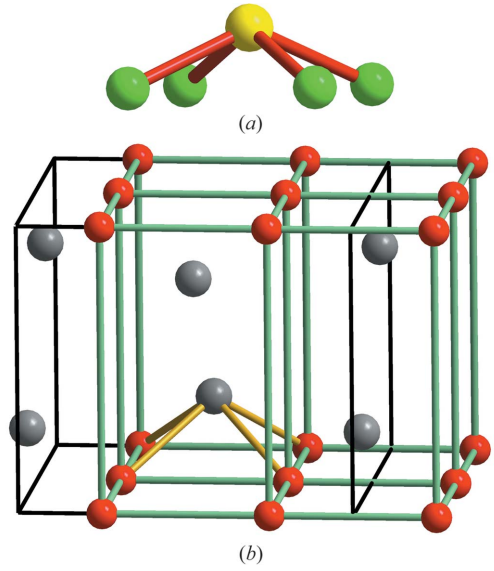

Figure 4
(*a*) The square-pyramidal structure of the SF_4 molecule. (*b*) The same array formed by the $[PbO_4]^{6-}$ subunit in the unit cell of red PbO. S: yellow; O: red; Pb: grey. Note that lone pairs linked to both S and Pb atoms occupy the apical positions of the pyramid.

of ELF have also been recently generalized to the treatment of correlated wavefunctions (Silvi, 2003; Kohout, 2004; Kohout *et al.*, 2004, 2005; Matito *et al.*, 2006; Wagner *et al.*, 2007; Feixas *et al.*, 2010). Comprehensive descriptions concerning the nomenclature associated with the topological analysis of this local function have been presented elsewhere (Silvi & Savin, 1994; Savin *et al.*, 1996; Silvi, 2002) and here we will only mention the relevant details necessary for completeness of the present study. The analysis of the *gradient field* or topology of ELF provides a partition of the molecular space into non-overlapping volumes or *basins* that are associated with entities of chemical significance as *atomic cores* and *valence regions* (*e.g.* bonds or lone pairs). Valence basins are in turn classified in terms of the number of core basins with which they share a boundary, *i.e.* the so-called *synaptic order* (Silvi, 2002). The average basin population in any basin i can be obtained by integrating the one-electron density probability $\rho(\mathbf{r})$ in such a region, $N_i = \int_i \rho(\mathbf{r})\,\mathrm{d}\mathbf{r}$.

Variances and delocalization indices are also introduced from the integration of the two-electron density probabilities in the ELF basins. Such a population analysis has been found to be a useful tool in rationalizing the *electron delocalization* in several molecular systems, providing deeper insight and understanding about the *nature of the chemical bonding* in a variety of both stationary and reacting systems. Examples include the analysis of pericyclic processes (Chamorro & Notario, 2004; Cárdenas *et al.*, 2005; Chamorro *et al.*, 2007), cycloaddition processes (Berski *et al.*, 2003; Domingo *et al.*, 2008), radical systems (Melin & Fuentealba, 2003) and aromaticity (Santos *et al.*, 2005).

The optimization of the molecular structures for all the compounds studied in this work has been carried out at the B3LYP/6−311++G(*d*,*p*) level of theory, performed with the *Spartan*'08 (Wavefunction Inc, 2009) and *GAUSSIAN*09 (Frisch *et al.*, 2009) series of programs. Each stationary structure was characterized as a minimum by analytical frequency calculations. The topological analysis of ELF has been carried out using the *TopMod* program (Noury *et al.*, 1997, 1999) and VMD visualization tools (Humphrey *et al.*, 1996, and version 1.9 for Windows, 2011), from the optimized wavefunctions at the B3LYP/6-311++G(*d*,*p*) level of theory.

3. Results and discussion

Theoretical calculations were carried out on the molecule $(H_3C)_3-Si-O-Si-(CH_3)_3$ (hexamethyldisiloxane). In this molecule the angular and the linear geometries are equally stable as deduced from the similar values of energy, with very small deviations among the different geometries. In both geometries there are three possibilities related to the position of the two $Si(CH_3)_3$ groups: eclipsed, staggered and intermediate (see Fig. 5). In all geometries the two Si−O distances are of *ca* 1.65 Å. The Si−O−Si angle in angular geometries is *ca* 170° (see Table 1). Angular and linear geometries of the $(H_3C)_3-Si-O-Si-(CH_3)_3$ molecule will be discussed next in separate sections.

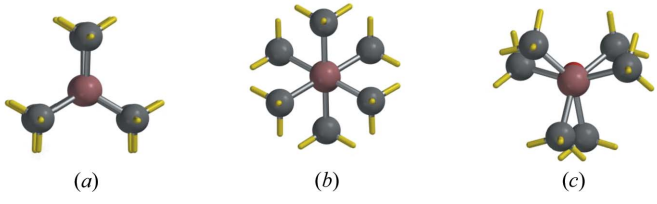

Figure 5
(*a*) Eclipsed, (*b*) staggered and (*c*) intermediate conformations of hexamethyldisiloxane.

Table 1
B3LYP/6-311++G(*d*,*p*)-optimized structures of $(H_3C)_3-Si-O-Si-(CH_3)_3$ (hexamethyldisiloxane).

Energies in Hartrees, Si−O distances in Ångstroms, and Si−O−Si angles in degrees.

Conformation	E_{el}†	E_0‡	Si−O	Si−O−Si
Angular				
Eclipsed	−894.018347 (0.1)	−893.793354 (2.3)	1.656	165.9
Staggered	−894.018331 (0.1)	−893.793989 (0.6)	1.655	168.0
Intermediate	−894.018368 (0.0)	−893.793682 (1.4)	1.654	170.9
Linear				
Eclipsed	−894.018286 (0.2)	−893.794203 (0.1)	1.654	180.0
Staggered	−894.018283 (0.2)	−893.794233 (0.0)	1.654	180.0
Intermediate	−894.018374 (0.0)	−893.793381 (2.2)	1.646	180.0

† Electronic energies. In parentheses, relative values in kJ mol^{-1}. ‡ Energies at 0 K, including zero-point vibrational energies calculated at the B3LYP/6-31G(*d*) level. In parentheses, relative values in kJ mol^{-1}.

3.1. The angular geometry of hexamethyldisiloxane

The topology of the electron localization domains has been represented by the ELF = 0.84 isosurfaces in all cases. The $(H_3C)_3-Si-O-Si-(CH_3)_3$ molecule in an angular geometry is represented in Fig. 6. A consistent picture of Si−O−Si bonding can be drawn from the ELF analysis: (*a*) three core basins which are associated with the Si and O atoms; (*b*) two disynaptic valence basins associated with the Si−O bond regions, with a population of 1.62 electrons in each one, in

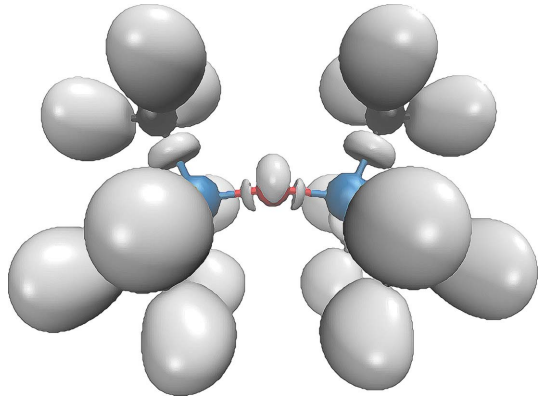

Figure 6
Localization domains of the electron localization function (ELF) at angular $(H_3C)_3-Si-O-Si-(CH_3)_3$ (as calculated at ELF = 0.84 isosurface) from the optimized wavefunction at the B3LYP/6-311++G(d,p) level of theory.

agreement with the existence of (2*e*, 2*c*) bonds; (*c*) three monosynaptic valence basins corresponding to the lone pair region of oxygen, which appear fused as a continuous bow covering a range of $\sim 120^{\circ}$, with a total population of 4.62 electrons.

This angular geometry is the most frequent in the related ether molecules as well as in saturated hydrocarbons like $H_3C-CH_2-CH_3$ and their similarity can be explained in terms of the isolobal character of O atoms and the CH_2 group, with the two O lone pairs playing the role of the two C—H bonds of the methylene group in propane. This interpretation is coincident with the VSEPR picture which places bonds and lone pairs on a comparable basis (Papoian & Hoffmann, 2000).

The importance of this interpretation, based on the isolobal concept (Hoffmann, 1982), is that it gives conceptual support to another qualitative approach, the anions in metallic matrices model (AIMM; Vegas *et al.*, 2006) that conceives a structure as formed by a skeleton of cations bonded by directed covalent bonds and where each O atom tries to catch two electrons when located in the vicinity of the bonding pairs. The advantage of this new approach with respect to the classical point of view is that it applies not only to molecules but also to extended solids. This has clearly been stated in the works of Vegas and co-workers concerning the structures of aluminates and silicates (Santamaría-Pérez & Vegas, 2003; Santamaría-Pérez *et al.*, 2005).

Recalling the AIMM model, it should be stressed that those comprehensive studies of the structures of aluminates and silicates led to conclude that the insertion of the O atoms at (or near) the middle point of the line joining the *X* atoms (*X* = Al, Si, P) was a universal feature. This alternative description of such structures shows that the O atoms are located in the vicinity of either bonding or lone pairs. In angular geometries, the O atoms deviate $\sim 0.3-0.4$ Å from the line of the *X*—*X* bonds. This feature was advanced when we discussed the $[Si_2P_6O_{25}]^{12-}$ polyanion in $In_4[Si_2P_6O_{25}]$ (Santamaría-Pérez *et al.*, 2005) (see Fig. 2). However, it should be recalled that in $In_4[Si_2P_6O_{25}]$ (see Fig. 2), both types of geometry are present. Thus, the O atoms bridging the Si and P atoms deviate from the bonding line, whereas the central O atom is co-linear with the two Si atoms, a trend that is observed in other molecular structures containing the Si—O—Si group that are collected in CSD (Allen, 2002).

In order to illustrate this phenomenon we will consider some additional pertinent examples like the structures of the P_4, P_4O_6 and P_4O_{10} molecules, which are compared in Fig. 7. Thus, when six O atoms approach the six edges of the P_4 tetrahedron, they catch the bond pairs involved in the P—P bonds, forming the P_4O_6 molecule. When additional O atoms are inserted, they locate close to the lone pairs forming the terminal P—O bonds observed in the oxides P_4O_7, P_4O_8, P_4O_9 and P_4O_{10} (see Fig. 5). Note that along the whole series of oxides the topology of the P_4 molecule is always preserved, a feature that repeats in various SiO_2 polymorphs (cristobalite, tridymite and keatite; O'Keeffe & Hyde, 1985; Santamaría-Pérez *et al.*, 2005). In all these binary oxides, the structural

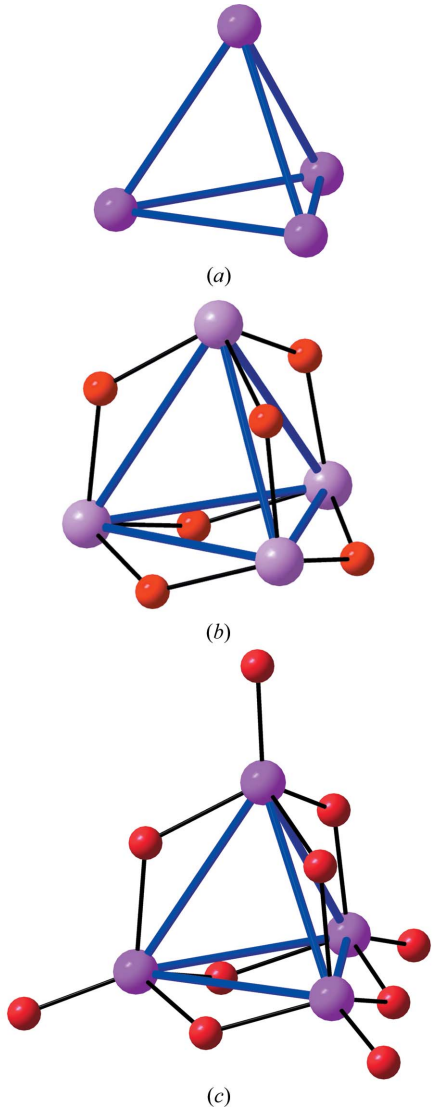

Figure 7
The structures of the P_4, P_4O_6 and P_4O_{10} molecules showing the angular array of the P—O—P groups. The P atoms are always connected with blue lines to outline the topology of the P_4 molecule (P: purple, O: red).

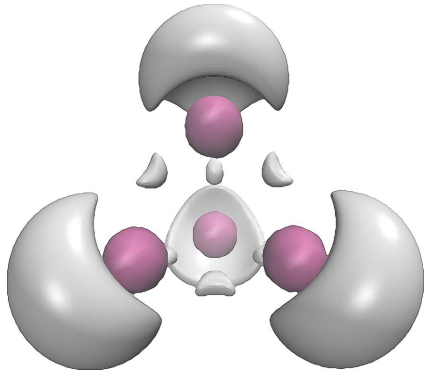

Figure 8
Localization domains of the ELF at P_4 (as calculated at ELF = 0.84 isosurface) from the optimized wavefunction at the B3LYP/6-311++G(d,p) level of theory.

result is a three-dimensional framework of corner-connected [XO_4] tetrahedra, centered by the X atom (Si, P). The most important feature is, however, that under these tetrahedral frameworks underlie the structures of the parent element (Si, P) thus giving additional support to the novel AIMM (Vegas *et al.*, 2006; Santamaría-Pérez & Vegas, 2003; Santamaría-Pérez *et al.*, 2005; Vegas & Mattesini, 2010). As will be discussed later, similar ideas were advanced by Bent (1965, 1966, 1968).

The topologies of the electron localization domains for the P_4 and P_4O_6 molecules are represented in Figs. 8 and 9. In P_4 (see Fig. 8) there are: (*a*) four core basins which are associated with the P atoms; (*b*) six disynaptic valence basins associated with the P—P bond regions, with a population of 1.23 electrons in each one, which are located out of the P—P line; (*c*) four monosynaptic valence basins corresponding to the lone pair region of the P atoms, with a population of 3.09 electrons in each one. Similarly, in P_4O_6 (see Fig. 9) there are: (*a*) ten core basins which are associated with the P and O atoms; (*b*) 12 disynaptic valence basins associated with the P—O bond regions, with a population of 1.50 electrons in each one; (*c*) four monosynaptic valence basins corresponding to the lone pair region of P atoms, with a population of 2.16 electrons in each one; (*d*) six monosynaptic valence basins corresponding to the lone pair region of O atoms, with a population of 4.74 electrons in each one. It is interesting to note that the six O atoms in P_4O_6 are located in the same positions where the six disynaptic valence basins associated with the P—P bond regions are located in P_4.

It has been suggested for a long time that in the tetrahedral P_4 molecule, the close P—P—P angles (60°) would produce a repulsion of the P—P bonding clouds. To minimize this repulsion, the P—P bonds would bend forming banana-like orbitals. Interestingly, the fact that the basins in P_4 are off the P—P bond lines agrees with this idea. This is also the reason why the O atoms in P_4O_6 deviate much more from the P—P line than the O atoms in the SiO_2 polymorphs. This feature has found support in the theoretical study of the topology of the electron density in P_4 clusters reported by Tsirelson *et al.* (2006), in which the bonding-critical points (BCPs) are out of the line connecting two P nuclei. Instead, the bonding points should be located on bent lines mimicking the banana-like orbitals mentioned above. The angle at the BCP is 170° and the position of the basin (see Fig. 7) is quite close to the position of the BCP calculated by Tsirelson *et al.* (2006). This lack of linearity is typical for the strained bonds, although the angle is more open than that calculated by Jones & Hohl (1990).

Consequently, the calculated P—O—P angle in P_4O_6 is *ca* 127°, closer than the Si—O—Si angle in the SiO_2 polymorphs

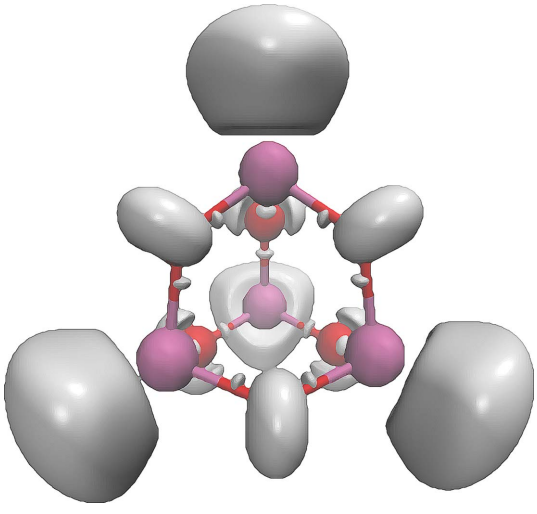

Figure 9
Localization domains of the ELF at P_4O_6 (as calculated at ELF = 0.84 isosurface) from the optimized wavefunction at the B3LYP/6-311++G(d,p) level of theory.

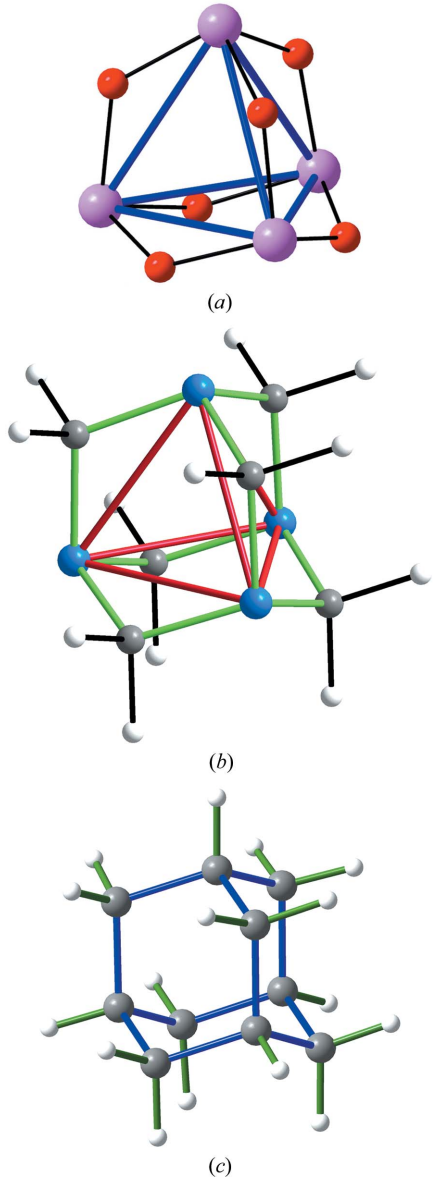

Figure 10
The molecular structures of the isolobal compounds: (*a*) P_4O_6, (*b*) hexamethylenetetramine (HMT) and (*c*) adamantane. In HMT the C—N bonds are drawn with green lines. In addition, the N atoms (blue) have been connected with red lines to identify the underlying structure of a hypothetical N_4 molecule similar to that of P_4 in P_4O_6.

(145–160°; Dollase, 1965; O'Keeffe & Hyde, 1981). Recall that in the elementary Si polymorphs, the Si—Si bonds are not bent.

What has been discussed for the P_4/P_4O_6 pair could be extended to the $P_4O_6/N_4(CH_2)_6$ (hexamethylenetetramine)/$(CH)_4(CH_2)_6$ (adamantane) trio. The reason for this comparison is the isolobal character of P, N and CH on one hand, and of O and CH_2 on the other. In this special case the three molecules are not only isolobal but also isoelectronic, and adopt similar skeletons as shown in Fig. 10. As far as we know, this is the first time that these three molecules have been interpreted on a common basis by AIMM (Vegas *et al.*, 2006).

3.2. The linear geometry of hexamethyldisiloxane

When the linear geometry is considered, the ELF calculations reveal quite a different situation. The topology of the electron localization domains for the $(H_3C)_3—Si—O—Si—(CH_3)_3$ molecule in a linear geometry is represented in Fig. 10. The ELF analysis presents: (*a*) three core basins which are associated with the Si and O atoms; (*b*) two disynaptic valence basins associated with the Si—O bond regions, with a population of 1.46 electrons in each one, in agreement with the existence of (2*e*, 3*c*) bonds; (*c*) three monosynaptic valence basins located in the equatorial plane, corresponding to the lone pair region of oxygen, which appear fused as a continuum toroidal distribution, with a total population of 4.90 electrons.

As can be seen in Fig. 11 two attractors appear in the line of the Si—O bonds, but are displaced towards the O atom. Their populations are lower than those observed in the angular molecule where the charge was estimated approximately in two electrons. This fact indicates that in the linear geometry, the bonding in the Si—O—Si group can be described as a (2*e*, 3*c*) bond in which the two electrons are provided by the two sp^3 hybrid orbitals of the two Si atoms containing one electron each. An empty *p* orbital of the O atom is also involved in the linear bond. If this were so, the six valence electrons of the O atoms would be paired in three lone pairs that would be located in the equatorial plane. In other words, it can be considered that the three lone pairs occupy the three sp^2 hybrid orbitals, playing the same role as the C—H bonds in (I^+), giving sense to the prediction of the VSEPR model (Gillespie & Popelier, 2001).

The ELF topology confirms the isolobal character of the O atom and the CH_3^+ moiety in the carbocation (I^+) (see Fig. 1). In other words, the linearity of the Si—O—Si group has a decisive influence on the location of the lone pairs attached to the O atom as does the linear Si—C—Si group in the trigonal bipyramidal coordination of the central C atom in the $[(H_3C)_3—Si—CH_3—Si—(CH_3)_3]^+$ carbocation (I^+) (Laskin *et al.*, 2000).

Another molecule, isoelectronic with both the CH_3^+ cation and the O atom, is the borane BH_3. For this reason, we have also extended our calculation to the hypothetical molecule $(H_3C)_3—Si—BH_3—Si—(CH_3)_3$, also isolobal with the carbocation (I^+). In this B-containing compound the most stable configuration is linear (Si—B—Si angle of 180.0°), but in this case the BH_3 moiety deviates slightly from planarity, with H—B—H angles of 118.6° and Si—B distances of 2.04 and 2.06 Å (see Fig. 12). This pyramidal geometry of the BH_3 group might induce different charge donation from the two $Si(CH_3)_3$ groups towards the BH_3 group. In fact, the populations of the two disynaptic valence basins associated with the Si—B bond regions are different, 0.98 and 1.47 electrons. This fact can be observed in Fig. 13.

An alternative geometry would be one where the BH_3 molecule forms an adduct with the $(H_3C)_3—Si—Si—(CH_3)_3$ molecule. In this case the two electrons of the Si—Si bond would be donated to the empty sp^3 orbital of BH_3, which would then adopt a pyramidal geometry. This was thought as possible in that the empty sp^3 orbital of the pyramidal BH_3

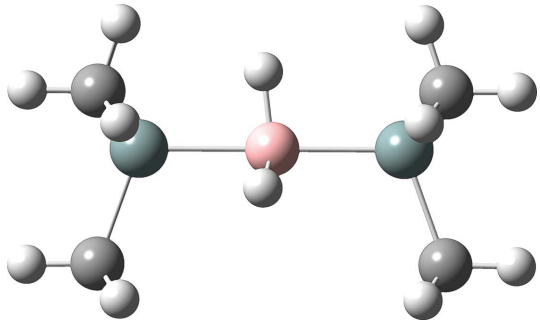

Figure 12
B3LYP/6-311++G(d,p)-optimized structure of $(H_3C)_3—Si—BH_3—Si—(CH_3)_3$.

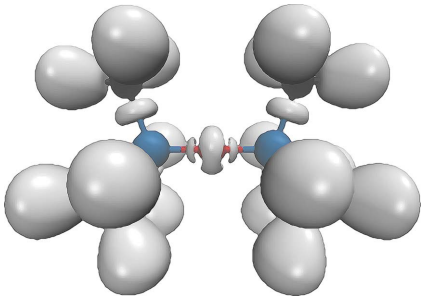

Figure 11
Localization domains of the ELF at linear $(H_3C)_3—Si—O—Si—(CH_3)_3$ (as calculated at ELF = 0.84 isosurface) from the optimized wavefunction at the B3LYP/6-311++G(d,p) level of theory.

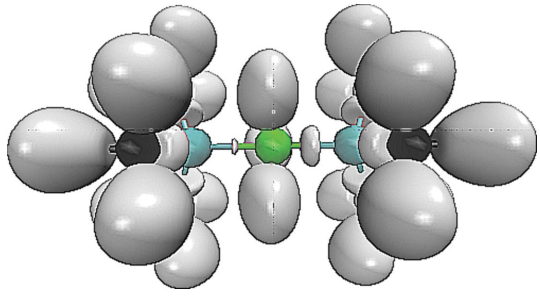

Figure 13
Localization domains of the ELF at linear $(H_3C)_3—Si—BH_3—Si—(CH_3)_3$ (as calculated at ELF = 0.84 isosurface) from the optimized wavefunction at the B3LYP/6-311++G(d,p) level of theory.

molecule might show a strong acidic character, forming an adduct compound where the donor pair is the two electrons of the Si—Si bond and leading to an angular geometry. Although at the calculation levels of this work the optimization of this geometry did not work, its existence should not be discarded.

4. Concluding remarks

4.1. Chemical considerations

We can conclude by saying that the calculations presented in this work confirm the idea that the O atom, when forming part of molecules like those described here, is isolobal with the isoelectronic CH_3^+ and BH_3 groups. We recognize that the isoelectronic comparison of O and BH_3 is not new, *e.g.* see diverse borane derivatives (Kodama & Parry, 1961; Carter & Parry, 1965; Riess & Van Wazer, 1967; Malone & Parry, 1967; Bent, 1966; Sergueev & Shaw, 1998). However, in all of these cases the oxygen is singly coordinated, *X*O *versus* *X*BH_3*X*, as opposed to dicoordinated *XOX versus* *X*BH_3*X*, as discussed here. We might also want to recall the transient formation of $(BH_3)^{2-}$ (analogous to O^{2-}) accompanied by $(B_2H_6)^{2-}$ (analogous to O_2^{2-}) in the reduction of B_2H_6 (Godfroid *et al.*, 1994), and the solution phase characterization of the radical anion $(B_2H_6)^{-\bullet}$ (Marti & Roberts, 1984) analogous to $O_2^{-\bullet}$. Indeed BH_3 and B_2H_6 additionally mimic atomic and diatomic oxygen. The oxygen trimer O3 and tetramer O4 are unstable oligomers (allotropes) of oxygen compared with O2. Related to this, both the trimer B_3H_9 and tetramer B_4H_{12} are unstable oligomers of BH_3 compared with B_2H_6. Indeed, pure O3 is explosive and O4, B_3H_9 and B_4H_{12} remain unisolated.

This vision of the molecular structures in which the O atoms, when approaching electron pairs (bond pairs and lone pairs) transform the electron density so that the skeletons of the elements are preserved in the oxides. We speculated previously (Santamaría-Pérez *et al.*, 2005) that some residual density could persist below the O atom in the angular P—O—P group in P_4O_6. The results we present here seem to be more consistent with the idea that the preservation of the elemental skeleton in the oxides is not due to any residual electron density in the line connecting the *X*—*X* bonds (*X* = P, Si, S *etc.*), but to expansion of the elemental network as a consequence of the formation of (2*e*, 3*c*) bonds.

We agree with Gillespie & Popelier (2001) that the bonding in the so-called 'hypervalent' molecules usually involving atoms of the elements of period 3 and beyond is not different in type from that in the related period 2 elements, and there is therefore little justification for the continued use of the 'hypervalency' concept (Gillespie & Popelier, 2001). In other words, our results clearly show that ligand lone-pair coordination number (LLPCN; Gillespie & Popelier, 2001) is also observed for atoms like C, O and B. If we make use of the equivalence between bonding and lone pairs mentioned above (Papoian & Hoffmann, 2000), we see that this LLPCN = 5 is not restricted to atoms larger than those from period 2. Thus, the explanation of this fact seems to be a consequence of the orbital models and not a question of the atomic size, as suggested by Gillespie & Popelier (2001).

Papoian & Hoffmann (2000) have discussed the structure of two Sb polyanions, *i.e.* Sb_3^{7-} and Sb_3^{5-}, in terms of hypervalency. Both polyanions are found in the solid state (Rehr & Kauzlarich, 1994; Sologub *et al.*, 1996). The 22 valence electron hypervalent structure Sb_3^{7-} prefers to be linear, while the 20 valence electron classical structure Sb_3^{5-} prefers to be bent, consistent with the isoelectronic molecule analogues XeF_2 and SF_2, respectively. The different geometry observed in these Sb polyanions could be accounted for by using the model discussed in this work.

This behavior does not differ from that shown by other linear molecules such as LiOLi (Büchler *et al.*, 1963; Rehm *et al.*, 1992; Lievens *et al.*, 1999; Schulz *et al.*, 1999; Sullivan *et al.*, 2003) and NaONa (Rehm *et al.*, 1992; Schulz *et al.*, 1999; Sullivan *et al.*, 2003), where hypervalency is absent; why CsOCs is bent (Buechler *et al.*, 1967; Spiker & Andrews, 1973) is not obvious. The question about the angular or linear geometries of such molecules, also including $H_3Si—O—SiH_3$ and $[H_3Al—F—AlH_3]^-$, was considered by Bent in the 60s (Bent, 1965, 1968), in the light of the tangent-sphere model.

The O atoms in the molecules we have studied in this work would play the same role as the formally present O^{2-} anions in the ionic bonds, connecting molecular and solid-state chemistry. This similarity is more evident when we compare these results with the experimental observations and theoretical calculations recently reported for some inorganic solids (Marqués *et al.*, 2009; Vegas & Mattesini, 2010). In the former, Marqués *et al.* (2009) reported the existence of a new high-pressure phase of potassium (*h*P4-K) whose structure is identical to the K-substructures in both the high-pressure phase of K_2S and in the high-temperature phase of K_2SO_4. The important issue is that calculations of the ELF show that, in *h*P4-K, the valence electrons (four per unit cell) are paired and located at the same positions as the S atoms in K_2S and in γ-K_2SO_4. Thus, classical anions mimic the valence electrons of elemental K which, in this phase, is an electride. Subsequent calculations of the ELF on the pairs Ca/CaO and BaSn/$BaSnO_3$ (Vegas & Mattesini, 2010) have provided additional evidence on how the valence electrons of the metals/alloys (Ca, BaSn) are located at the same place as the O atoms in the oxides.

We now return to $[(H_3C)_3—Si—CH_3—Si—(CH_3)_3]^+$ and $[(H_3C)_3—Si—BH_3—Si—(CH_3)_3]$ with linear Si—*X*—Si (*X* = C and B) substructures and put these 'exotic' species into more classical chemical context. These have eight valence electrons and so may be recognized as a class of species ignored in the earlier qualitative molecular orbital treatment of non-transition metal, but otherwise general AB_5 species even though most species of this type have 10 or 12 valence electrons (Gimarc, 1978). Nonetheless, we will use the correlation diagram and other analyses found in this study.

Let us start by simplifying our discussion by replacing the two trimethyl silyl groups by simple univalent substituents that bond only through a single σ orbital. Doing so results in a trigonal bipyramidal species with four valence orbitals that are

all doubly occupied, the lower two are nondegenerate, the higher two are a degenerate pair. Squeezing the two equatorial H atoms again splits the double degeneracy and would be expected to result in destabilization much as is found in planar AH_3 and AB_3 species upon distortion from D_{3h} to C_{2v} symmetry (Gimarc, 1971). Opening the angle between two equatorial H atoms en route to a square-pyramidal geometry again splits the double degeneracy and raises the energy as seen from the above AB_5 and AH_3 references alike.

We also recognize $[(H_3C)_3-Si-CH_3-Si-(CH_3)_3]^+$ as a disubstituted derivative of protonated methane, CH_5^+. This last species does not have a D_{3h} geometry with a linear H—C—H assemblage. Literature quantum chemical calculations show that some $CH_3M_2^+$ ions prefer a linear $M-C-M$ assemblage (Jemmis *et al.*, 1979), a situation we expect to be facilitated by 'large' M groups such as our $(H_3C)_3Si$ group simply for steric reasons.

Deprotonation of the central CH_3 group in principle allows for mixing of the various orbitals because of reduced symmetry. In turn the Si—C—Si angle can shrink from 180° and this gives us a disilylated methane, *i.e.* the normal species $(H_3C)_3-Si-CH_2-Si-(CH_3)_3$. This has a much more conventional structure, however, one with an enlarged Si—C—Si angle (*ca* 123°) compared with most other disubstituted methanes. This was ascribed to steric repulsion of the silyl groups. However, all of the same reasons that encourage linearity for $[(H_3C)_3-Si-CH_3-Si-(CH_3)_3]^+$ should be applicable, resulting in this large angle (Fjeldberg *et al.*, 1983). Further deprotonation is quite facile, *i.e.* $(H_3C)_3-Si-CH_2-Si-(CH_3)_3$ is quite acidic. The anion (as well as the corresponding radical) $(H_3C)_3-Si-CH^*-Si-(CH_3)_3$ is stabilized for both scenarios, * = (−) and • (Brinkman *et al.*, 1994; Römer *et al.*, 1998).

We do not expect to be able to affect the deprotonation of $[(H_3C)_3-Si-CH-Si-(CH_3)_3]^-$ to form the free (unsolvated, unmetallated) dianion $[(H_3C)_3-Si-C-Si-(CH_3)_3]^{2-}$. However, isoelectronic to this dianion is the disiloxane $(H_3C)_3-Si-O-Si-(CH_3)_3$ and the weakly basic hexamethyldisilazide anion $[(H_3C)_3-Si-N-Si-(CH_3)_3]^-$. We note that the dilithiated (and however ionic, nonetheless neutralized) dianion $(H_3C)_3-Si-CLi_2-Si-(CH_3)_3$ has been observed (Kawa, Chinn & Lagow, 1984; Kawa, Manley & Lagow, 1984).

It has been suggested from gas-phase ion-energetics measurements (Higgins *et al.*, 2001) that $[(H_3C)_3-Si-N-Si-(CH_3)_3]^-$ is linear but readily lithiated in solution to form a markedly bent species. All of these findings are in agreement with electronic and structural flexibility expressed in terms of the facile interconversion of a conventional structure and our new one in which a two-electron, three-centre description is most valid.

4.2. Crystallographic considerations

A special comment should be made on the experimental and conceptual features that lead us to unite the role of bridged O atoms in both the hexamethyldisiloxane molecule $(H_3C)_3-Si-O-Si(CH_3)_3$ and in the silicates, as well as the silica polymorphs. The book 'Structural Chemistry of Silicates' (Liebau, 1985), Table 3.3, provides a few examples of compounds exhibiting a linear (or almost linear) Si—O—Si fragment. Liebau (1985) highlights two important features common to all these compounds: (1) 'in general, the amplitude of vibration of the bridging O atoms is greater than those of the terminal O atoms'; (2) 'in general, the amplitudes of vibration of the bridging atoms are much higher in a direction within or near a plane perpendicular to the Si···Si vector' ... 'the thermal ellipsoid of the O atom clearly demonstrates that this atom prefers to vibrate in directions at right angles to the Si···Si vector'. Since in standard crystal structure determinations the final refinement makes use of all the structure factors, the obtained thermal ellipsoids may not necessarily reflect the image of the true thermal vibration amplitudes, but they are significantly influenced by the asphericity of the valence electron density due to both bonding and lone pairs.

Such asphericity normally produces an increase in the thermal amplitudes as well as a change in the shape of the ellipsoids. These changes can be important in atoms such as O atoms where more than 50% of the valence electrons are located at the lone-pair regions. Crystallographers are aware that reliable thermal amplitudes can only be obtained either from neutron diffraction data, as it is the case of the mineral petalite discussed below (Tagai *et al.*, 1982), or from high-angle X-ray reflections where the contribution of the valence electrons is insignificant. In the latter case under the assumption that careful corrections by extinction, absorption, multiple diffraction and thermal diffuse scattering (TDS) are required.

Because this is the case of the bridging O atoms in silicates, the observation of Liebau (1985) regarding both the magnitude and the shape of the ellipsoids is consistent with the results of the ELF calculations reported here. Thus, the disk-shaped ellipsoids of the bridging O atom can be correlated with the ELF values observed in the equatorial plane of the disiloxane molecule. Thus, the lentil-shaped basin depicted in Fig. 11 must necessarily have a decisive influence on the thermal parameters obtained from X-ray data and collected by Liebau (1985). The issue can be summarized as follows: *The shape of the thermal ellipsoids for the central O atom, as derived from the X-ray structure determinations, are not only an indication of a preferred vibration of that atom in the plane perpendicular to the Si–Si vector but also that the electron density around the central O atom is distributed as a disc or lentil as shown in the ELF. In the standard structure determinations both features are inseparable*.

This issue puts in front of us another feature which has not been considered so far. In silicate structures containing linear Si—O—Si groups, the bridging O atom bonds only to the two Si atoms but not to any other atom of the structure. Thus, in $Sc_2[Si_2O_7]$ (tortveitite), the central O atom of the linear Si—O—Si group (see Fig. 2*c*) is not in the coordination sphere of the Sc atoms. In $LiAl[Si_4O_{10}]$ (petalite; Tagai *et al.*, 1982), the $[AlSi_4O_{10}]^1$-subnet forms a tetrahedral four-connected XO_2 (X = Al, Si) network in which the XO_4 tetrahedra share all corners forming both linear and angular (163°) $X-O-X$

groups. The important outcome here is, however, that all the O atoms are involved in the coordination sphere of the Li atoms, with the exception of O1 which is just the central atom of the linear Si—O—Si groups.

A similar situation occurs in the dimorphic mineral $BaFe[Si_4O_{10}]$ (gillespite). Above 1.8 GPa the compound is orthorhombic ($P2_12_12$) (Hazen & Finger, 1983), with all the Si—O—Si bonds angular and where all the bridging O atoms are coordinated to the Ba atoms. Below 1.8 GPa, the compound is tetragonal ($P4/ncc$) (Hazen & Finger, 1983) and the structure contains angular ($\angle$ at O = 150°) groups coexisting with almost linear Si—O—Si ($\angle$ at O = 178°) arrays. In this case, however, the O atoms of the linear groups are not coordinated to either Fe or Ba atoms. The same feature is also observed in $Ca_6[Si_6O_{17}](OH)_2$ (xonotlite; Hejny & Armbruster, 1979) and in $Er_2[Si_2O_7]$ (Smolin & Shepelev, 1968).

The above description indicates that O atoms involved in linear arrays satisfy their valence requirements by bonding uniquely to the two Si atoms. In other words, if the central O atom captures the bonding pair of a Si—Si bond, it also satisfies the octet rule that forms the (2*e*, 3*c*) bond of Fig. 11. This might prevent further coordination to any other atom by means of the three lone-pair (LP) electrons attached to the central O atom. The question that arises is whether the delocalization of the LP electrons (see Fig. 11), which can also be inferred from the thermal ellipsoids, might also cause this behaviour. Contrarily, in the angular geometry the LP electrons are well localized, thus allowing for coordination to additional atoms other than Si. The fact that both types of geometries occur in SiO_2 and silicates as well as in the disiloxane molecules seems to indicate that the 'fragment-within-the-solid' concept, discussed above, is also applicable to these compounds.

Species such as (I^+) lead to speculation on the possibility of transitions of similar molecules to solid-state cages in which linear groups such as Si—O—Si, Si—CH_2—Si and Si—BH_3—Si might coexist forming extended solids with new properties. The substitution of the bridging oxygen in the $[Si_2O_7]^{6-}$ pyrosilicate anion (see Fig. 2*c*), which in fact is a fragment of the tridymite structure (SiO_2), as well as the reported insertion of acidic centers in saponite (Xue & Pinnavaia, 2010), could serve as examples of this idea.

4.3. Final conceptual synthesis assertions

Our final comment should remark that the idea of considering O atoms as equivalent to electron pairs, which motivated this work and that have been restricted as yet to classical ionic compounds (Santamaría-Pérez & Vegas, 2003; Santamaría-Pérez *et al.*, 2005; Vegas *et al.*, 2006), can also be extended to molecules. This is one of the main points of our work, *i.e.* to outline that a bonding pair involved in a (2*c*, 2*e*) Si—Si bond is an attractor for an O atoms in order to satisfy its octet. When inserted, this O atom can be notionally seen as an O^{2-} formal anion, but simultaneously it is also involved in the (3*c*, 2*e*) bond of the Si—O—Si group. Moreover, this (3*c*, 2*e*) bond also implies charge sharing between Si and O forming covalent Si—O bonds. As stated in the title of this work, this study not only concerns the isoelectronic and isolobal character of O, CH_2, CH_3^+ and BH_3, but also their role *as electron pairs*.

The relevance of our model has been manifested in several of our previous works. Thus, Vegas & Jansen (2002) reported more than 100 examples of oxides whose cation arrays have the same structure as the corresponding alloy, with the O atoms always moving following the transitions of the cations trying to locate in the vicinity of electron pairs (either LP or BP). This idea that connects lone pairs, bonding pairs and O atoms, later extended to ionic compounds such as K_2S and CaO (Vegas & Mattesini, 2010), helps us to understand other structural features which are not explained by classical ionic concepts. To illustrate this behaviour we will provide several examples:

One is the disulfide K_2S_2 that forms a distorted NiAs-type structure (Böttcher *et al.*, 1993), which is preserved by the K_2S_2 subarray in the corresponding oxide $K_2(S_2O_6)$ (de Matos Gomes *et al.*, 1996). The similarity of both structures is observable in Fig. 14 and the reason for that is quite simple: in K_2S_2 the S atoms are forming the $[S—S]^{2-}$ dianions with the S atoms bonded by a single σ bond. The result is that each S atom has three terminal lone pairs forming a tetrahedral geometry with the bonding pair. When the dianions are oxidized, the six LP electrons are converted into the six S—O bonds in $K_2(S_2O_6)$ which are represented in Fig. 14(*b*).

Following the same reasoning, one can imagine how, starting from a thiosulfate group S—SO_3, the sequence O_2S—SO_3, O_3S—SO_3 and O_3S—O—SO_3 can be formed by a gradual insertion of O atoms where LP electrons and O atoms seem play a similar structural role.

Another interesting example is provided by the pair of compounds Na_2S/Na_2SO_4 (Vegas & García-Baonza, 2007). Na_2SO_4 undergoes three phase transitions (V) → (III) → (II) → (I)-Na_2SO_4 on increasing the temperature. The last one occurs at 543 K and will be discussed next. (I)-Na_2SO_4 is hexagonal ($P6_3/mmc$) with the same space group as the high-pressure phase of the sulfide Na_2S. One of the Na atoms forms infinite 3^6 layers parallel to the *ab* plane. Contrarily, the second Na and the S atoms form infinite graphene-like sheets intercalated with the Na-3^6 layers. The important issue here is that the SO_4 groups show rotational disorder, a fact which is normally attributed to the thermal motion caused by the high temperature. It is noteworthy that in the other two high-temperature phases (463 and 493 K) the O atoms are located at fixed positions.

Opposite to this feature is the case of $ZnSO_4$ which is distorted NiAs-type under ambient conditions. When heated at 973 K (a temperature much higher than that of Na_2SO_4), the compound becomes cristobalite-type, where the ZnS subarray adopts the zincblende structure, just the structure of the binary alloy ZnS itself. However, in this compound, the O atoms are not disordered but **fixed** at the middle of the Zn—S bonds.

As far as we know, a physical interpretation of the different behaviour shown by both compounds has not been reported

so far. However, our model can account for this order–disorder problem on the basis of the equivalence between LP electrons and O atoms. Thus, if we assume that the Na atoms forming the 3^6 layers transfer their valence electron to the Na/S pair forming the graphitic layers, the result is a $[Na_3S_3]^{3-}$ anionic planar net, which can be regarded as Ψ-Mg_3S_3, a Ψ-(II)–(VI) compound which like in other cases can form a structure similar to the (IV)–(IV) compounds. If this were so, the graphite-like layers should have an aromatic character leading to the delocalization of part of the electron cloud and hence to the impossibility of fixing the O atoms.

This model also accounts for the localization of the O atoms in HT-$ZnSO_4$. At 973 K when the ZnS subarray forms the cubic zincblende structure [again a (II)–(VI) compound adopting a (IV)–(IV) structure], the formation of directed Zn—S bonds is assumed and then the O atoms locate in the vicinity of these directed bonds. Electrons are not disordered like in Na_2SO_4! It is the first time that thermal disorder is interpreted in a rational way.

A third example can be found in the new crystal chemistry of aluminates and silicates reported by Santamaría-Pérez & Vegas (2003) and Santamaría-Pérez *et al.* (2005), where, for the first time, thousands of compounds (aluminates, silicates, phosphates, germanates, *etc.*) can be explained on the basis of a unique concept, *i.e.* the extended Zintl–Klemm concept applied to cation in oxides, implying that the O atoms move towards the located pairs of electrons.

We acknowledge that the calculations carried out in the present work have much in common and, indeed, find strong support in old ideas expressed by Bragg, recalled by Bent (1965, 1966, 1968). In our opinion the central essence is that '*molecules are not built of atoms, molecules are built of atomic cores and electride ions. The whole molecule is one small crystal*'. Bent's ideas are much more far reaching when saying that '*many of the rules of crystal chemistry may be applied to covalent compounds*'. Thus, the counterpart of Pauling's First Rule of Crystal Chemistry can be expressed in the case of molecules as: '*In molecules a coordinated polyhedron of electride ions is formed about each atomic core*'. According to Lewis (1923, 1938), Sidgwick & Powell (1940), and Gillespie & Nyholm (1957), Bent established a Second Rule of Covalent Chemistry, expressed as: '*Structurally, lone pairs may often be treated like bonding pairs*' (Bent, 1968). These are just the results we have reported previously (Santamaría-Pérez & Vegas, 2003; Santamaría-Pérez *et al.*, 2005) and which have been presented here.

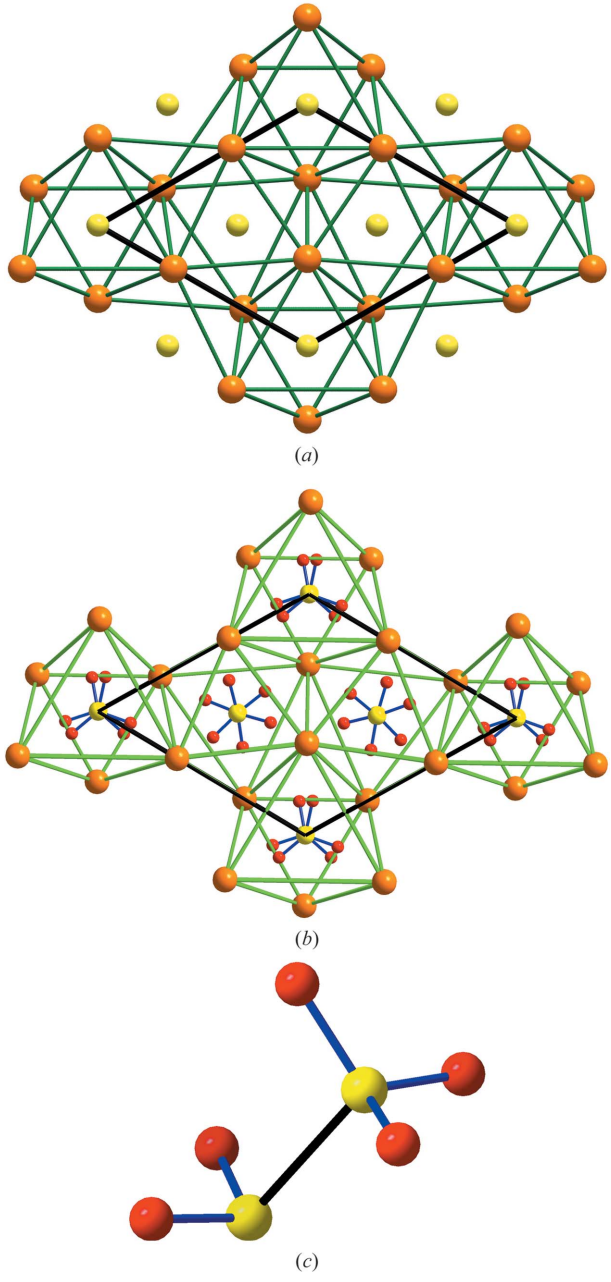

Figure 14
(*a*) The hexagonal structure of K_2S_2 projected onto the *ab* plane, forming a distorted NiAs-type array. The K atoms are in hexagonal close packing (h.c.p.) with the S atoms occupying all the octahedral voids. (*b*) The trigonal structure of $K_2S_2O_6$ projected onto the *ab* plane. The h.c.p. array of the K atoms shows greater distortion by the inclusion of the O atoms. K: brown; S: yellow; O: red. The S_2O_6 groups are in both eclipsed and almost staggered configurations. (*c*) The isolated $[O_2S—SO_3]^{2-}$ anion as an intermediate step between $S—SO_3$ and $O_3S—SO_3$.

This work is dedicated to Professor Henry A. Bent on the occasion of his 85th birthday as a tribute to his pioneering work connecting molecular structures and solid-state chemistry. RN and JFL give thanks to the Spanish Ministerio de Ciencia e Innovación under Project CTQ2010-16402 for financial support. EC and PP acknowledge support from FONDECYT-Chile grants 1100277 and 1100278; and from UNAB through project NUCLEO DI-219-12.

References

Allen, F. H. (2002). *Acta Cryst.* B**58**, 380–388.
Allen, L. C. & Burdett, J. K. (1995). *Angew. Chem. Int. Ed.* **34**, 2003–2004.
Becke, A. D. & Edgecombe, K. E. (1990). *J. Chem. Phys.* **92**, 5397–5403.
Bent, H. A. (1965). *J. Chem. Educ.* **42**, 348–354.
Bent, H. A. (1966). *J. Chem. Educ.* **43**, 170–186.
Bent, H. A. (1968). *J. Chem. Educ.* **45**, 768–778.

Berski, S., Andrés, J., Silvi, B. & Domingo, L. R. (2003). *J. Phys. Chem. A*, **107**, 6014–6024.
Brinkman, E. A., Berger, S. & Brauman, J. I. (1994). *J. Am. Chem. Soc.* **116**, 8304–8310.
Böttcher, P., Getzschmann, J. & Keller, R. (1993). *Z. Anorg. Allg. Chem.* **619**, 476–488.
Büchler, A., Stauffer, J. L., Klemperer, W. & Wharton, L. (1963). *J. Chem. Phys.* **39**, 2299–2303.
Buechler, A., Stauffer, J. L. & Klemperer, W. (1967). *J. Chem. Phys.* **46**, 605–608.
Burdett, J. K. & Lin, J.-H. (1981). *Acta Cryst.* B**37**, 2123–2132.
Burdett, J. K. & Lin, J.-H. (1982). *Acta Cryst.* B**38**, 408–415.
Cárdenas, C., Chamorro, E. & Notario, R. (2005). *J. Phys. Chem. A*, **109**, 4352–4358.
Carter, J. C. & Parry, R. W. (1965). *J. Am. Chem. Soc.* **87**, 2354–2358.
Chamorro, E. E. & Notario, R. (2004). *J. Phys. Chem. A*, **108**, 4099–4104.
Chamorro, E., Notario, R., Santos, J. & Pérez, P. (2007). *Chem. Phys. Lett.* **443**, 136–140.
Cruickshank, D. W. J., Lynton, H. & Barclay, G. A. (1962). *Acta Cryst.* **15**, 491–498.
Dávalos, J., Herrero, R., Abboud, J., Mó, O. & Yáñez, M. (2007). *Angew. Chem. Int. Ed.* **46**, 381–385.
Dewar, M. J. S. & Ford, G. P. (1979). *J. Am. Chem. Soc.* **101**, 783–791.
Dollase, W. A. (1965). *Z. Kristallogr.* **121**, 369–377.
Domingo, L. R., Chamorro, E. & Pérez, P. (2008). *J. Org. Chem.* **73**, 4615–4624.
Feixas, F., Matito, E., Duran, M., Solà, M. & Silvi, B. (2010). *J. Chem. Theor. Comput.* **6**, 2736–2742.
Fernández, I., Uggerud, E. & Frenking, G. (2007). *Chem. Eur. J.* **13**, 8620–8626.
Fjeldberg, T., Seip, R., Lappert, M. F. & Thorne, A. J. (1983). *J. Mol. Struct.* **99**, 295–302.
Frisch, M. J. *et al.* (2009). *GAUSSIAN*09, Revision A.02. Gaussian, Inc., Wallingford, CT, USA.
Gillespie, R. J. & Nyholm, R. S. (1957). *Q. Rev. Chem. Soc.* **11**, 339–380.
Gillespie, R. J. & Popelier, L. A. (2001). *Chemical Bonding and Molecular Geometry. From Lewis to Electron Densities.* New York: Oxford University Press.
Gimarc, B. M. (1971). *J. Am. Chem. Soc.* **93**, 593–599.
Gimarc, B. M. (1978). *J. Am. Chem. Soc.* **100**, 2346–2353.
Godfroid, R. A., Hill, T. G., Onak, T. P. & Shore, S. G. (1994). *J. Am. Chem. Soc.* **116**, 12107–12108.
Hanawa, M., Kobayashi, T. & Imoto, H. (2000). *Z. Anorg. Allg. Chem.* **626**, 216–222.
Hazen, R. M. & Finger, L. W. (1983). *Am. Mineral.* **68**, 595–603.
Hejny, C. & Armbruster, T. (1979). *Mineral. J*, **9**, 349–373.
Higgins, P. R., Hinde, R., Grimm, D. T., Bloor, J. E. & Bartmessa, J. E. (2001). *Int. J. Mass Spectrom.* **210/211**, 231–240.
Hoffmann, R. (1982). *Angew. Chem. Int. Ed.* **21**, 711–724.
Hoffmann, R., Shaik, S. & Hiberty, P. C. (2003). *Acc. Chem. Res.* **36**, 750–756.
Humphrey, W., Dalke, A. & Schulten, K. (1996). *J. Mol. Graph.* **14**, 33–38.
Jemmis, E. D., Chandrasekhar, J. & Schleyer, P. v. R. (1979). *J. Am. Chem. Soc.* **101**, 527–533.
Jones, R. O. & Hohl, D. (1990). *J. Chem. Phys.* **92**, 6710–6721.
Kawa, H., Chinn, J. W. Jr & Lagow, R. J. (1984). *J. Chem. Soc. Chem. Commun.* pp. 1664–1665.
Kawa, H., Manley, B. C. & Lagow, R. J. (1988). *Polyhedron*, **19/20**, 2023–2025.
Klevan, L. & Munson, B. (1974). *Int. J. Mass Spectrom. Ion Phys.* **13**, 261–268.
Kodama, G. & Parry, R. (1961). *J. Inorg. Nucl. Chem.* **17**, 125–129.
Kohout, M. (2004). *Int. J. Quantum Chem.* **97**, 651–658.
Kohout, M., Pernal, K., Wagner, F. R. & Grin, Y. (2004). *Theor. Chem. Acc.* **112**, 453–459.
Kohout, M., Pernal, K., Wagner, F. R. & Grin, Y. (2005). *Theor. Chem. Acc.* **113**, 287–293.
Laskin, J., Byrd, M. & Futrell, J. (2000). *Int. J. Mass Spectrom.* **195/196**, 285–302.
Leclaire, A., Lamire, M. & Raveau, B. (1988). *Acta Cryst.* C**44**, 1181–1184.
Lewis, G. N. (1923). *Trans. Faraday Soc.* **19**, 452–458.
Lewis, G. N. (1938). *J. Franklin Inst.* **226**, 293–313.
Liebau, F. (1985). *Structural Chemistry of Silicates: Structure, Bonding and Classification.* Berlin: Springer-Verlag.
Lievens, P., Thoen, P., Bouckaert, S., Bouwen, W., Vanhoutte, F., Weidele, H., Silverans, R. E., Navarro-Vázquez, A. & Schleyer, P. V. R. (1999). *J. Chem. Phys.* **110**, 10316–10329.
Malone, L. J. & Parry, R. W. (1967). *Inorg. Chem.* **6**, 817–822.
Marqués, M., Ackland, G. J., Lundegaard, L. F., Stinton, G., Nelmes, R. J., McMahon, M. I. & Contreras-García, J. (2009). *Phys. Rev. Lett.* **103**, 115501.
Marti, V. P. J. & Roberts, B. P. (1984). *J. Chem. Soc. Chem. Commun.* pp. 272–274.
Matito, E., Silvi, B., Duran, M. & Solà, M. (2006). *J. Chem. Phys.* **125**, 024301.
Matos Gomes, E. de, Ortega, J., Etxebarría, J., Zúniga, F. J. & Breczewski, T. (1996). *J. Phys. Condens. Matter*, **8**, 2063–2071.
Melin, J. & Fuentealba, P. (2003). *Int. J. Quantum Chem.* **92**, 381–390.
Messmer, R. P., McCarroll, B. & Singal, C. M. (1972). *J. Vac. Sci. Technol.* **9**, 891–897.
Messmer, R. P. & Watkins, G. D. (1973). *Radiation Damage and Defects in Semiconductors.* London: Institute of Physics.
Moore, W. J. & Pauling, L. (1941). *J. Am. Chem. Soc.* **63**, 1392–1394.
Mootz, D. & Korte, L. (1984). *Z. Naturforsch. B*, **39**, 1295–1299.
Noury, S., Krokidis, X., Fuster, F. & Silvi, B. (1997). *TopMod*. Université Pierre et Marie Curie, Paris, France.
Noury, S., Krokidis, X., Fuster, F. & Silvi, B. (1999). *Comput. Chem.* **23**, 597–604.
O'Keeffe, M. & Hyde, B. G. (1981). *Structure and Bonding in Crystals*, edited by M. O'Keeffe & A. Navrotsky, Vol. I. New York: Academic Press.
O'Keeffe, M. & Hyde, B. G. (1985). *Struct. Bond.* **61**, 77–144.
Papoian, G. & Hoffmann, R. (2000). *Angew. Chem. Int. Ed.* **39**, 2408–2448.
Rehm, E., Boldyrev, A. I. & Schleyer, P. v. R. (1992). *Inorg. Chem.* **31**, 4834–4842.
Rehr, A. & Kauzlarich, S. M. (1994). *J. Alloy. Compd.* **207/208**, 424–426.
Riess, J. G. & Van Wazer, J. R. (1967). *J. Am. Chem. Soc.* **89**, 851–856.
Römer, B., Gatev, G. G., Zhong, M. & Brauman, J. I. (1998). *J. Am. Chem. Soc.* **120**, 2919–2924.
Santamaría-Pérez, D. & Vegas, A. (2003). *Acta Cryst.* B**59**, 305–323.
Santamaría-Pérez, D., Vegas, A. & Liebau, F. (2005). *Struct. Bond.* **118**, 121–177.
Santos, J. C., Andres, J., Aizman, A. & Fuentealba, P. (2005). *J. Chem. Theor. Comput.* **1**, 83–86.
Savin, A., Becke, A. D., Flad, J., Nesper, R., Preuss, H. & von Schnering, H. G. (1991). *Angew. Chem. Int. Ed.* **30**, 409–412.
Savin, A., Nesper, R., Wengert, S. & Fässler, T. F. (1997). *Angew. Chem. Int. Ed.* **36**, 1808–1832.
Savin, A., Silvi, B. & Coionna, F. (1996). *Can. J. Chem.* **74**, 1088–1096.
Schön, J. C. (1995). *Angew. Chem. Int. Ed.* **34**, 1081–1083.
Schulz, A., Smith, B. J. & Radom, L. (1999). *J. Phys. Chem. A*, **103**, 7522–7527.
Sergueev, D. S. & Shaw, B. R. (1998). *J. Am. Chem. Soc.* **120**, 9417–9427.
Sidgwick, N. V. & Powell, H. M. (1940). *Proc. R. Soc. Lond. A*, **176**, 153–180.
Silvi, B. (2002). *J. Mol. Struct.* **614**, 3–10.
Silvi, B. (2003). *J. Phys. Chem. A*, **107**, 3081–3085.
Silvi, B. & Savin, A. (1994). *Nature*, **371**, 683–686.
Smolin, Y. N. & Shepelev, Y. F. (1968). *Inorg. Mater.* **4**, 992–995.

Sologub, O., Vybornov, M., Rogl, P., Hiebl, K., Cordier, G. & Woll, P. (1996). *J. Solid State Chem.* **122**, 266–272.
Spiker, R. C. Jr & Andrews, L. (1973). *J. Chem. Phys.* **58**, 713–721.
Stone, A. J. (1997). *Mass Spectrom. Rev.* **16**, 25–49.
Sullivan, M. B., Iron, M. A., Redfern, P. C., Martin, J. M. L., Curtiss, L. A. & Radom, L. (2003). *J. Phys. Chem. A*, **107**, 5617–5630.
Tagai, T., Ried, H., Joswig, W. & Korekawa, M. (1982). *Z. Kristallogr.* **160**, 159–170.
Tsirelson, V. G., Tarasova, N. P., Bobrov, M. F. & Smetannikov, Y. V. (2006). *Heteroat. Chem.* **17**, 572–578.
Wavefunction Inc (2009). *Spartan 08*, Version 1.1.1. Wavefunction Inc., Irvine, CA, USA.
Vegas, Á. & García-Baonza, V. (2007). *Acta Cryst.* B**63**, 339–345.
Vegas, Á. & Jansen, M. (2006). *Acta Cryst.* B**58**, 38–51.
Vegas, Á. & Mattesini, M. (2010). *Acta Cryst.* B**66**, 338–344.
Vegas, Á., Santamaría-Pérez, D., Marqués, M., Flórez, M., García Baonza, V. & Recio, J. M. (2006). *Acta Cryst.* B**62**, 220–227.
Wagner, F. R., Bezugly, V., Kohout, M. & Grin, Y. (2007). *Chem. Eur. J.* **13**, 5724–5741.
Wojtyniak, A. C. M., Li, X. & Stone, J. A. (1987). *Can. J. Chem.* **65**, 2849–2854.
Xue, S. & Pinnavaia, T. J. (2010). *Appl. Clay Sci.* **48**, 60–66.
Zunger, A. (1974*a*). *J. Phys. C*, **7**, 76–95.
Zunger, A. (1974*b*). *J. Phys. C*, **7**, 96–106.
Zunger, A. (1975). *Ann. Soc. Sci. Brux. Ser. 1*, **89**, 231–251.